J Mater Sci: Mater Med (2006) 17: 573–581
DOI 10.1007/s10856-006-8942-2

Bioactive ceramic composites sintered from hydroxyapatite and silica at 1200°C: preparation, microstructures and *in vitro* bone-like layer growth

X. W. Li · H. Y. Yasuda · Y. Umakoshi

Received: 30 March 2005 / Accepted: 9 August 2005

Abstract Bioceramic composites were synthesized by sintering the powders of hydroxyapatite (HAp) mixed directly with additive of 0.5, 1.0, 2.0, 5.0 and 10 wt.%SiO_2, respectively, at 1200°C. X-ray diffraction (XRD) analysis indicated that the phase transformation from HAp to tricalcium phosphate (TCP) comprising α-TCP and Si-TCP occurred and became more prominent with the addition of SiO_2 and the increase in SiO_2 content. The observations of their surface microstructures showed that the addition of SiO_2 suppressed the grain growth and promoted the formation of crystalline-glassy composites denoted HAp + TCP/Bioglass. As the SiO_2 content is as high as 5 wt.%, the composite made a feature of crystalline clusters with different sizes consisting of HAp and TCP grains surrounded by the matrix of glassy phase. Furthermore, the dependence of in vitro bioactivity of these composites on the SiO_2 content was biomimetically assessed by determining the changes in surface morphology, i.e., bone-like apatite layer growth, after soaking in an acellular stimulated body fluid (SBF) for 3 days at 36.5°C. It was found that the HAp-SiO_2 composites showed a much faster bone-like layer growth than pure HAp, and the propensity of composites to exhibit a better bioactivity was getting more notable with increasing SiO_2 content, except for the case of the highest content of 10 wt.%. It was believed that the formation of the bone-like layer on the surfaces of these biocomposites is closely related to the increasingly provided silanol groups and transformed TCP phase in materials associated with the content of SiO_2 added.

X. W. Li (✉) · H. Y. Yasuda · Y. Umakoshi
Division of Materials Science and Manufacturing, Graduate School of Engineering, Osaka University, 2-1, Yamada-oka, Suita, Osaka 565-0871, Japan
Tel.: +81-6-6879-7527
e-mail: xwli@mat.eng.osaka-u.ac.jp or xwli6988@hotmail.com (X. W. Li)
e-mail: hyyasuda@mat.eng.osaka-u.ac.jp (H.Y. Yasuda)
e-mail: umakoshi@mat.eng.osaka-u.ac.jp (Y. Umakoshi)

X.W. Li
Institute of Materials Physics and Chemistry, College of Sciences, Northeastern University, Shenyang 110004, People's Republic of China

H. Y. Yasuda
Research Center for Ultra-High Voltage Electron Microscopy, Osaka University, 7-1, Mihogaoka, Ibaraki, Osaka 567-0047, Japan

1. Introduction

Different kinds of materials such as ceramics, polymers, transplanted cells and bioactive molecules have been used to regenerate bone in combination with some novel techniques [1]. As an ideal medical implant material, the synthetic calcium phosphate ceramic of hydroxyapatite (HAp) has been given the most common investigations since the major mineral constituent of such an osteoconductive and biocompatible material is quite similar to that of human hard tissues [1–4]. However, notwithstanding that new bone can form along the surfaces of either porous or dense HAp, the practically medical applications of HAp are still greatly restricted, since HAp is too stable in vivo to be absorbed and substituted by a new bone and the bone conductive effect is thus limited [5–7].

An earlier work by Carlisle [8], which reported that silicon (up to 0.5 wt.%) is often localized in active growth areas (*e.g.* the osteoid) of the young bone of mice and rats, has demonstrated the importance of silicon for bone formation and calcification. Many of recent investigations on bioactive glasses

and glass ceramics indicated that apatite layers could form on the surface of those materials after soaking in stimulated body fluid (SBF) and the silanol groups in those materials act as catalysts for the formation of bone-like apatite layers [9–16], which further revealed the significant effect of silicon on bone formation. Seeing that silicon is one of critical elements for the bone regeneration, and that trace element of silicon in calcium phosphate (Ca-P) ceramics or coatings can bring about an evident influence on the biological response as well as crystallographic, mechanical and chemical properties of implant materials [9], several investigators [17–24] have made attempts to elucidate the effect of addition of silicon (Si) or silica (SiO_2) on the sintering behavior of HAp by using different synthetic routes. For instances, over a much wider range of SiO_2 additions in HAp powders fired at 1100°C, Ruys [17] processed Si-substituted HAp using tetraethyl orthosilicate ($Si(OC_2H_5)_4$, TEOS) as a silicon source and found an impurity silicocarnotite ($Ca_5(PO4)_2{\cdot}SiO_4$) phase in HAp at the lowest SiO_2 additions accompanied by gradually increasing amounts of α-tricalcium phosphate (α-TCP), β-TCP and a Ca-Si-P-O amorphous phase with increasing content of SiO_2 added. However, based on investigations of Si-substituted HAp similarly using TEOS as the additive, Kim *et al.* [18, 19] reported that Si-substituted HAp containing 2 wt.% Si keep its original structure intact for the sintering temperatures of up to 1200°C, and the single-phase HAp containing silicon formed with non-existence of extra phases related to silicon oxide or other calcium phosphate species. Another important work has been done by Gibson *et al.* [20, 21], who adopted silicon acetate ($Si(CH_3COOH)_4$ as a source of up to 1.6 wt.% silicon and noted that the phase composition remained as HAp with no secondary phases such as TCP or CaO being formed, and no obvious change took place in the symmetry of the HAp crystallographic unit cell but small variations in lattice constants. Quite recently, several investigators [22–26] have studied systematically the preparation, phase composition and phase evolution in the silicon-stabilized tricalcium phosphate/apatite system by firing a stoichiometric HAp precipitate to which silicon was added. A commonly significant finding is that the resultant phase composition included a distinctive phase of silicon stabilized TCP (Si-TCP), which is a novel form of TCP stabilized by the substitution of silicon in tetrahedral phosphorus sites and has a monoclinic structure with the same crystalline space group ($P2_1/a$) as α-TCP but with characteristically different lattice parameters from α-TCP.

Apparently, all the aforementioned experimental efforts and analyses strongly indicated that the (trace) element of silicon could play an extremely important role in bone regeneration, and that incorporation of silicon into HAp could cause an obvious change in phase structure and composition. In the present study, bioceramic composites of SiO_2-added HAp with different amounts of SiO_2 were produced by sintering directly the mixtures of HAp and silica at 1200°C. The main objective is to reveal the effects of the content of SiO_2 additive on the phase composition and microstructures of such composites and explore the corresponding bone-like apatite layer growth features on the surfaces of these materials in stimulated body fluid (SBF), which is least investigated but is of practical significance for the application of such biocomposites in bone remolding.

2. Experimental

Pure HAp powder (HAP-100, Taihei Chemical Industry Co.) and colloidal silica dispersed in water (Nissan Chemical Industry Co.) were mixed in a ball mill together with ZrO_2 balls and ethanol. After mixing for 24 hrs, the powders were dried and sifted through a 60 mesh sieve. Since the particle diameter of colloidal silica is $10 \sim 20$ nm, uniformly mixed powders composed of HAp and SiO_2 could be obtained by using this method. In this way, a series of SiO_2-added HAp (HAp-SiO_2) powders containing 0.5, 1.0, 2.0, 5.0 and 10 wt.% SiO_2, respectively, were prepared. After preparation, these powders were calcined at 600°C for 2 hrs.

Disk-shaped pellets of HAp containing different amounts of SiO_2 were produced by pressing uniaxially the processed powders in a 6 mm diameter steel die. The green pellets were sintered at 1200°C for 2 hrs with heating and cooling rates of 100 °C/h. To identify the phase composition and content, X-ray powder diffraction measurements were made on each sintered sample using a Shimadzu XRD-6000S diffractometer. Cu Kα radiation was adopted at the operating condition of 40 kV and 30 mA. The XRD data were obtained over 2θ range of 10–70°at a step size of 0.01°.

After being sintered, one surface of the sample was mechanically grinded firstly by #2000 emery paper and then polished by 6 μm diamond paste. Subsequently, the polished samples were thermally etched at 1050°C for 2 hrs or chemically etched in 0.2 M lactic acid for several seconds. Prior to observing the microstructures in a scanning electron microscopy (SEM), the etched surfaces of samples were sputter-coated with a thin electrical conductive layer of gold-palladium alloy to avoid charging in the SEM.

After the sintered samples were mechanically grinded by #2000 emery paper, an in vitro bone-like layer growth test was performed by soaking the samples (sample size $\sim$28.3 mm^2) at 36.5°C in 30 ml of SBF in polyethylene bottles for 3 days with stirring but without refreshing the solution. The chemical compositions and pH of the SBF (vs. human blood plasma) are given in Table 1. The detailed preparation of SBF was described by Kokubo *et al.* [27]. After soaking, the features of bone-like layer formed on the sample surfaces were carefully examined by means of SEM.

Table 1 Ion concentrations and pH of the SBF solution compared to those of the human blood plasma (HBP)

	Ion Concentration (mM)								
	Na^+	K^+	Mg^{2+}	Ca^{2+}	Cl^-	HCO_3^{2-}	HPO_4^{2-}	SO_4^{2-}	pH
SBF	142.0	5.0	1.5	2.5	148.8	4.2	1.0	0.5	7.40
HBP	142.0	5.0	1.5	2.5	103.0	27.0	1.0	0.5	7.20–7.40

3. Results and discussions

3.1. Phase identification by X-ray diffraction

X-ray diffraction patterns of sintered samples of pure HAp and HAp-SiO_2 composites are shown in Fig. 1. It can be seen that the composition of the sintered pure HAp yielded a diffraction pattern that well matched the standard for HAp [4]. Upon addition of SiO_2 the phase transformation from HAp to TCP occurred and such a transformation became more marked with increasing content of SiO_2. X-ray diffraction analysis implied that the TCP phase is probably α-TCP phase, since all the diffraction peaks of TCP phase correspond to those of typical α-TCP phase. However, the existing results [25, 26] have demonstrated that firing of pure HAp in the presence of SiO_2 easily forms a unique crystalline Si-TCP phase ($Ca_3(P_{0.9}Si_{0.1}O_{3.95})_2$), which has a monoclinic structure with the same space group $P2_1/a$ as α-TCP. The α-TCP can transform to Si-TCP provided silicon added is sufficient [26]. Therefore, the present TCP phase should be a combination of α-TCP and Si-TCP phases. The following reactions were suggested to account for the phase transformation of HAp to TCP after sintering. Firstly, the decomposition of HAp occurred by the reaction

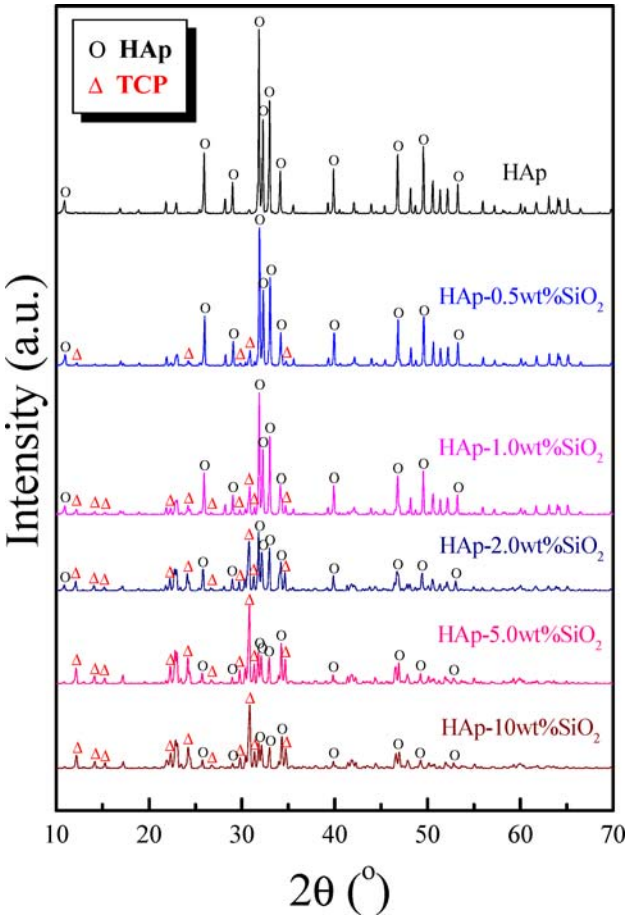

Fig. 1 X-ray diffraction patterns of pure HAp and HAp-SiO_2 containing different amounts of SiO_2 sintered at 1200°C for 2 hrs.

$$Ca_{10}(PO_4)_6(OH)_2 \rightarrow 3Ca_3(PO_4)_2 + CaO + H_2O \quad (1)$$

where $Ca_3(PO_4)_2$ is an α-TCP phase, which can subsequently be transformed to Si-TCP phase in combination with SiO_2 according to the following reaction:

$$10Ca_3(PO_4)_2 + 2SiO_2 \rightarrow 10Ca_3(P_{0.9}Si_{0.1}O_{3.95})_2 + P_2O_5 \quad (2)$$

These two reactions above will process simultaneously, and the reaction products of CaO and P_2O_5 might move to SiO_2 to form a typical bioactive glass, i.e. Ca-Si-P-O amorphous (glassy) phase, which has also been reported by other work [17, 25]. Here, the integral decrease in relative intensity of all diffraction peaks of each group of materials with increasing SiO_2 content, as shown in Fig. 1, indicated clearly the formation of an amorphous phase with a gradually increasing content.

To determine the wt.% of crystalline components of HAp and TCP in HAp-SiO_2 composites, a quantitative XRD analysis was adopted according to the following procedures: a set of reference samples was firstly made by mixing and homogenizing the powders of standard HAp and α-TCP with known wt.% of α-TCP, i.e., 20%, 40%, 60% and 80%. From XRD data of this set of samples we can then deduce the relationship between the ratio of integrated intensity of α-TCP at 2θ of 30.6° to that of HAp at 25.8° ($I_{30.6}/I_{25.8}$) and wt.% of α-TCP (W) as follows:

$$I_{30.6}/I_{25.8} = 13.998\,W^2 - 0.9753\,W \quad (3)$$

The indices of X-ray peaks at 25.8° and 30.6° are 002 for HAp and 034 for α-TCP, respectively. In this way, the ratio of

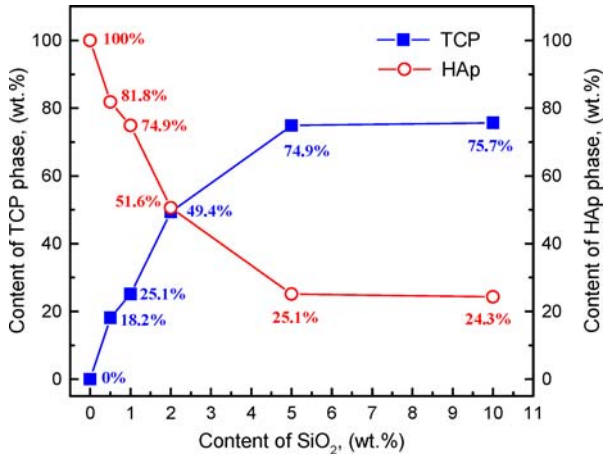

Fig. 2 Variation of phase composition of the crystalline components of HAp and TCP with the content of silicon added.

$I_{30.6}/I_{25.8}$ of each sintered sample of HAp-SiO_2 composites was measured from the XRD data, and then the wt.% of crystalline phases can easily be obtained based on the formula (3). It must be pointed out that, although the current TCP phase includes two phases of α-TCP and Si-TCP, the standard α-TCP was substituted for TCP as a reference material, since Si-TCP has a quite similar structure with α-TCP and the XRD profile of Si-TCP is thus almost identical with α-TCP. The corresponding results were depicted in Fig. 2. Apparently, the transformation of HAp to TCP became more pronounced as the content of SiO_2 added increased, and the crystalline phases present have switched from predominantly HAp to predominantly TCP at SiO_2 content of 2 wt.%. For example, approximately 75% of the crystalline phase of HAp has been converted to TCP phase when the SiO_2 content is as high as 5 wt.%.

As stated above, sintering stoichiometric HAp precipitates with different amounts of SiO_2 at 1200°C produced bioceramic composites consisting of crystalline phases (HAp and TCP) and a glassy component (Ca-Si-P-O). With the increase in SiO_2 content, the wt.% of transferred TCP from HAp increased notably, and an amorphous phase, i.e., bioglass, was simultaneously formed and its content increased in competition with the crystalline phases. Here, this produced material can thus be denoted as HAp+TCP/Bioglass.

3.2. Microstructural change with SiO_2 content

The effect of SiO_2 content on the sintered microstructures of materials was studied firstly by thermal etching, and the individually representative features of HAp and HAp-SiO_2 samples observed by SEM are presented in Fig. 3. Micrograph for the pure HAp indicated clear demarcation in grain boundaries and an average grain size could be readily estimated to be around 1–3 μm. With the addition of SiO_2 and an increase in SiO_2 content, the grain boundaries became gradually vague and the grain size decreased, as shown in Fig. 3 (b-d). This phenomenon was most discernable in the case of 2.0 wt.% (see Fig. 3 (d)). Despite the fact that the average grain size of HAp-SiO_2 samples was smaller than that for pure HAp, due to the addition of SiO_2, the microporosity in the microstructure was found to become greater (see Fig. 3 (b-d)), if compared with pure HAp, which was almost full dense (see Fig. 3 (a)).

On investigating effect of silicon substitution on the microstructure of HAp using silicon acetate ($Si(CH_3COOH)_4$ as a source of silicon, Gibson *et al.* [21] measured the activation energies of grain growth for HAp and Si-HAp samples. The measurements showed that the activation energy for HAp was about 141 kJ/ mol, whereas the corresponding values were higher than 180 kJ/ mol for Si-HAp samples, convincingly indicating a tangibly different gain growth kinetic of HAp and Si-HAp samples. Therefore, they concluded that the silicon substitution inhibited grain growth, so that for a given sintering temperature of 1200°C, the Si-HAp ceramics had significantly smaller grain sizes than stoichiometric HAp ceramics. It should be pointed out that, in their work, the phase composition of sintered Si-HAp samples was found to be solely made of HAp phase and no secondary phases, such as TCP, were observed for any of the different levels of silicon substitution at 1200°C. In the present work, when the SiO_2 content is lower than 2.0 wt.%, HAp is the prominent crystalline phase in spite of the existence of TCP phase, as shown in Fig. 2. Accordingly, under these circumstances, the principal features of observed microstructures in the present work are quite similar with the results by Gibson *et al.* [21], i.e., a decreasing grain size with increasing SiO_2 (or Si) content.

As the SiO_2 content increased to 5.0 wt.%, the role that HAp and TCP in the crystalline phase were playing changed and the TCP phase dominated the phase composition, meanwhile, the content of glassy phase, i.e., bioglass, increased. The microstructure of the HAp-5.0 wt.%SiO_2 sample exhibited quite distinctive characteristics, as typically seen in Fig. 3(e), which showed a bimodal structure, i.e., crystalline clusters of different sizes surrounded with glassy phase. The individual crystalline cluster consisted of HAp and TCP crystallites. The crystallites with smaller size and brighter contrast, as indicated by arrow 1 in Fig. 3(e), were thought to be HAp grains, since the grain size of HAp crystal decreased with increasing SiO_2 content, as aforementioned. By contrast those with comparatively greater size, as indicated by arrow 2 in Fig. 3(e), were naturally believed to be TCP grains.

Fig. 3(f) shows the microstructure of the sample with the highest SiO_2 content of 10 wt.%. The presence of glassy phase, whose content increased greatly, has made the GBs difficult to differentiate in compositions so that the

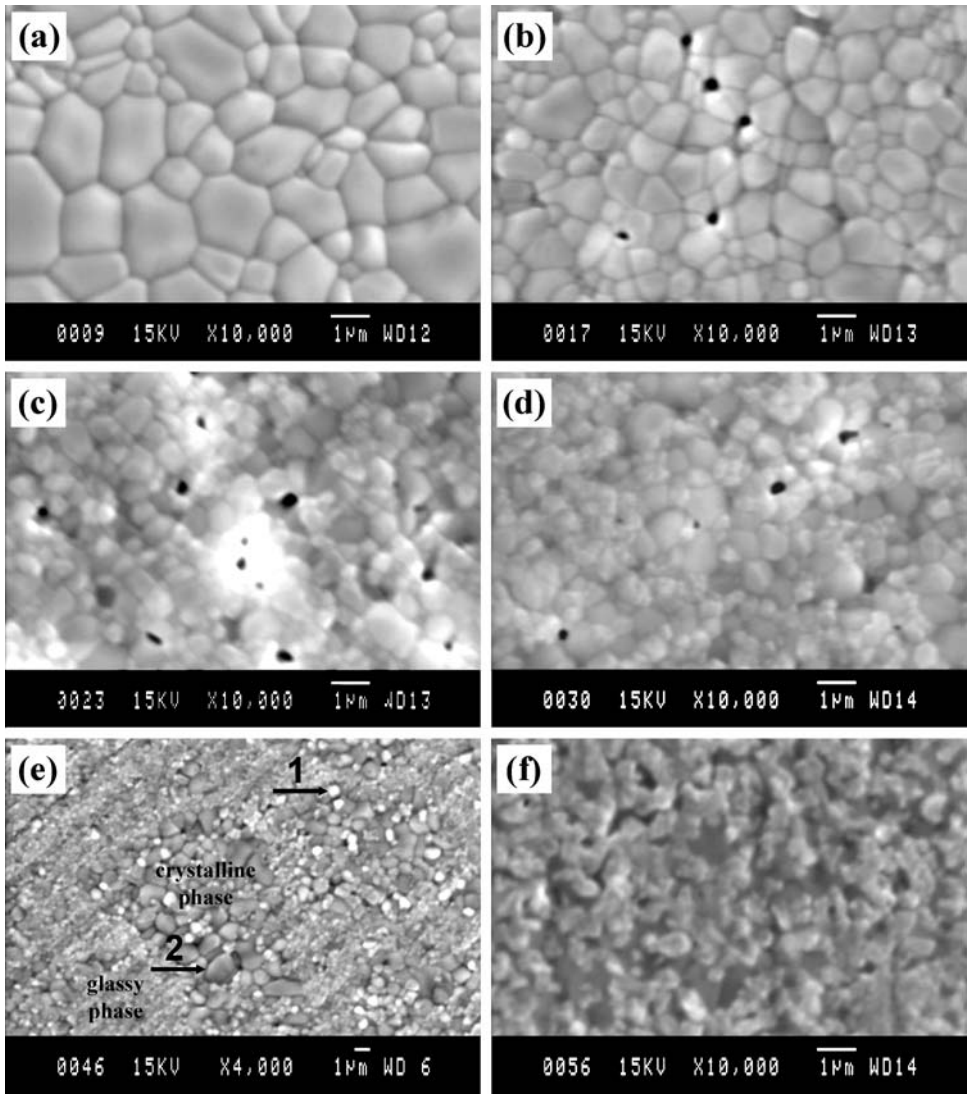

Fig. 3 SEM micrographs showing the effects of silicon content on the microstructures of sintered samples of (a) HAp, (b) HAp-0.5 wt.%SiO_2, (c) HAp-1.0 wt.%SiO_2, (d) HAp-2.0 wt.%SiO_2, (e) HAp-5.0 wt.%SiO_2, and (f) HAp-10 wt.%SiO_2, thermally etched at 1050°C for 2 hrs.

crystalline clusters observed in the sample containing 5.0 wt.% SiO_2 did not appear, except that a number of separated or interconnected crystalline particles with different sizes can be found to form in the matrix of glassy phase.

Fig. 4 shows the microstructure of the HAp-5.0 wt.%SiO_2 sample revealed by using chemical etching. From Fig. 4(a) it seems that the microstructure is composed of many inhomogeneous grains with different sizes and boundaries with different widths. In fact, these grains should correspond to the crystalline clusters indicated in Fig. 3(e) and the boundaries consist mainly of glassy phase. Due to the partial dissolution of crystalline phases of TCP and HAp into chemical solution of 0.2 M lactic acid, the real grain boundaries of these crystalline phases cannot be well shown except for the boundaries between crystalline and glassy phases. A magnified morphology of boundaries between crystalline and glassy phases was presented in Fig. 4(b), from which it can be seen that the crystalline morphology appeared to comprise rounded and interconnected particles of average size of 1.0 μm with a certain degree of porosity between the particles. This morphology is quite similar to that of Si-HAp ceramic pellets observed by Langstaff *et al.* [22]. The microstructures of other samples manifested by the chemical etching (data not shown here) are basically identical with those revealed by the thermal etching.

In light of the microstructures revealed by the aid of thermal and chemical etching methods, one can clearly note that crystalline-glassy composites formed with the addition of SiO_2, especially in the case that the SiO_2 content is as high as 5.0 wt.%, the composite appeared in the form of crystalline clusters with different sizes consisting of HAp and TCP grains surrounded by the matrix of glassy phase (HAp+TCP/Bioglass), as schematically shown in Fig. 5.

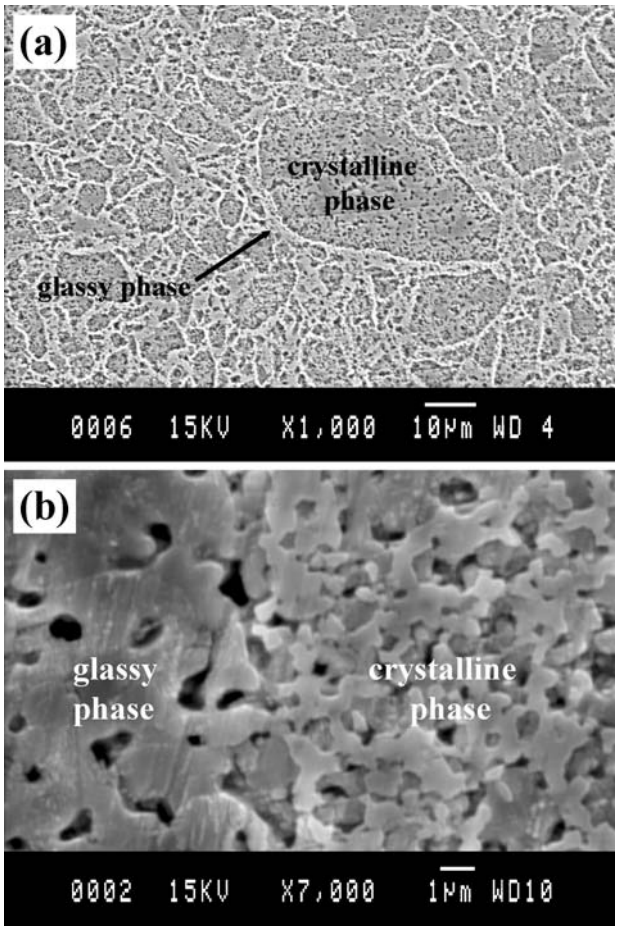

Fig. 4 SEM micrographs showing the microstructures of sintered HAp-5.0 wt.%SiO_2 sample chemically etched in 0.2 M lactic acid. (a) low magnification and (b) high magnification.

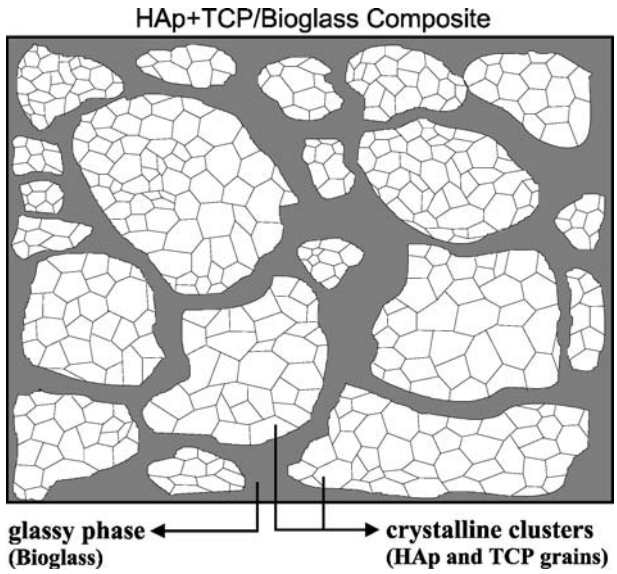

Fig. 5 A sketch of microstructures of HAp+TCP/Bioglass composite.

3.3. Formation of bone-like layer by soaking in SBF

Fig. 6 indicates the growth feature of bone-like layer on the surfaces of sintered HAp and HAp-SiO_2 samples in stimulated body fluid. It is apparent that the formation of bone-like layer on the sample surfaces is closely related with the SiO_2 content.

Firstly it should be mentioned that all the sintered samples were just mechanically grinded by #2000 emery paper to keep a certain surface roughness before immersion in the SBF. From Fig. 6(a) one can notice that there are merely few bone-like crystals with plate-like and particle shapes formed on the surface of HAp sample in local areas, and the scratches induced by mechanical grinding can be still clearly seen on the surface. Fig. 6(b) gives a high-magnification image of the plate-like crystals. It was found that these plate-like crystals were made of many ultra-fine grains with the size of about 100 nm. The basically similar surface feature was found for the sample of HAp-0.5 wt.%SiO_2 except that the bone-like crystals nearly covered the surface and the scratches became fainter, as shown in Fig. 6(c). Identically the bone-like crystals have ultra-fine (about 100 nm) grains (see Fig. 6(d)). These results strongly demonstrated that the addition of trace SiO_2 into HAp has been able to enhance markedly the in vitro bone-like apatite forming ability of materials.

As the SiO_2 content increased to 1.0 wt.%, there is an obvious change in the surface feature, as shown in Fig. 6(e). The entire surface of the sample was completely covered with the bone-like apatite layer and the scratches thus disappeared thoroughly. The formed apatite layer consisted numerous petal-like crystallites, as typically shown in Fig. 6(f), which is quite similar to that found on the surfaces of glass-ceramic A-W [28], Ceravital-type glass-ceramic [29] and Ca50Si50 glass [30]. On the petal-like apatite layer some spherical apatite particles with sizes ranging from 2 to 10 μm nucleated, and these particles were also made of many fine petal-like crystallites (see Fig. 6(e)). As the SiO_2 content further increased to 2.0 wt.%, a parallel feature is that the petal-like apatite layer covered fully the surface, whereas the differences are that numerous bone-like apatite particles have aggregated to form on the layer and that the size of petal-like apatites somewhat increased, as seen in Figs 6(g) and (h), indicating clearly a faster bone-forming speed on this material than on the sample containing 1.0 wt.% SiO_2.

For the sample of HAp-5.0 wt.%SiO_2, the surface characteristic after soaking in SBF exhibited diversity, but the most significant point is the formation of many well-developed spherical or round apatite crystallites with grain sizes ranging from 1 to 6 μm in local areas (see Fig. 6(i)). These apatite crystallites nucleated independently without common boundaries among them. Viewing the features as a whole, the obviously different three layers were found to form on

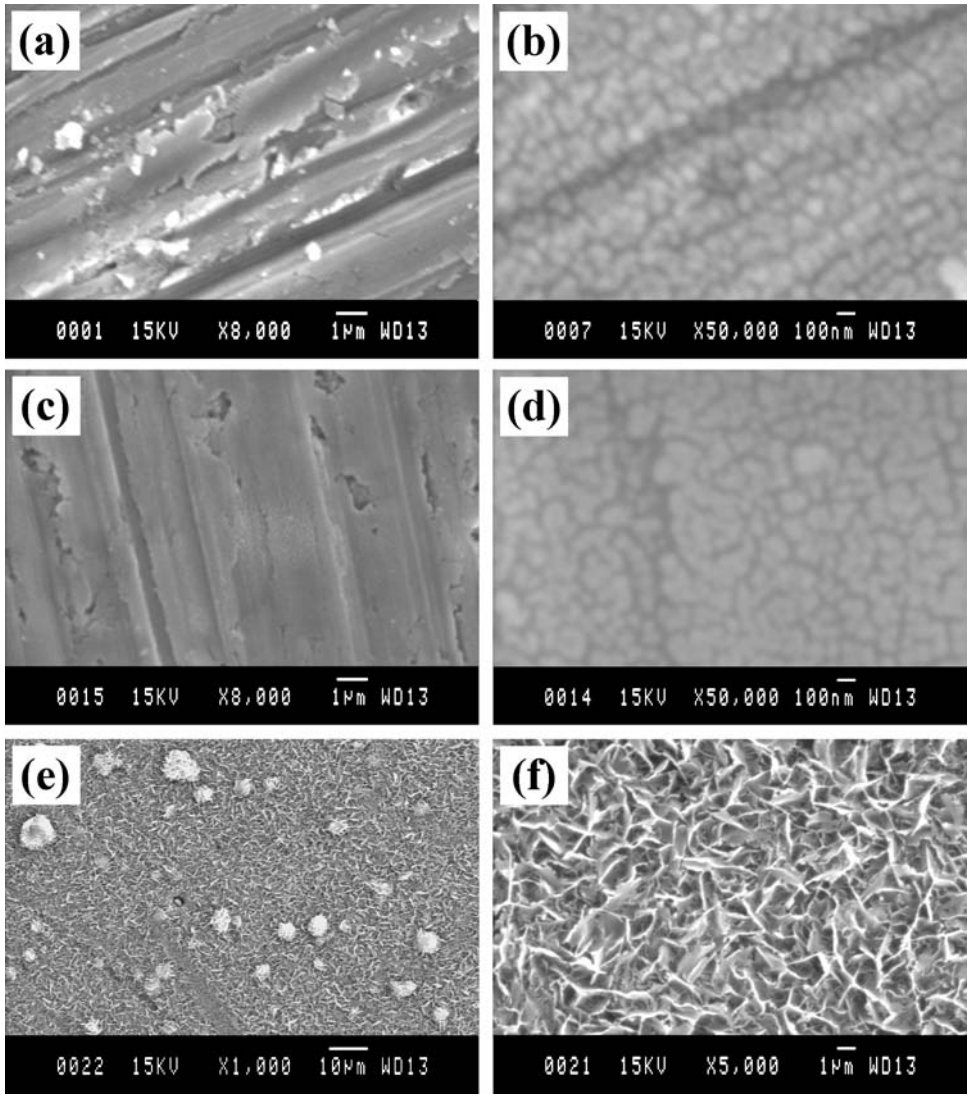

Fig. 6 SEM micrographs illustrating the surface features of samples of (a, b) HAp, (c, d) HAp-0.5 wt.%SiO_2, (e, f) HAp-1.0 wt.%SiO_2, (g, h) HAp-2.0 wt.%SiO_2, (i, j) HAp-5.0 wt.%SiO_2, and (k, l) HAp-10 wt.%SiO_2, sintered at 1200°C and then soaked in SBF solution for 3 days at 36.5°C.

the surface, i.e., (1) the first layer of small-size petal-like apatites, as indicated by area 1 in Figs 6(j); (2) the second layer of large-size petal-like apatites with some spherical bone-like apatite particles being formed (area 2 in Figs 6(j)) and (3) the top layer of well-developed apatite crystallites (area 3 in Fig. 6(j)). It is believed that the inhomogeneous formation of bone-like layers on this material is bound up with its unique microstructure indicated in Figs 3(e) and 5 as well as the inhomogeneous distribution of Ca^{2+} concentration on the surface.

From the results above it is evident that the increase in the SiO_2 content accelerates greatly the in vitro growth of bone-like layer on the surface of materials. However, it seems that the bone-layer growth become slower on the contrary, as the SiO_2 content reaches 10 wt.%, as shown in Fig. 6(k) and (l). Although there are many newly formed bone-like apatite crystals with plate-like or particle shapes on the surface, this bone-like layer is apparently quite thin because the scratches were still kept distinguishable, showing a slower bone formation on this material, as compared with other HAp-SiO_2 samples.

Kokubo *et al.* [11, 31] pointed out that the prerequisite for apatite formation on an artificial material in a living body is the presence of a type of functional groups that could be an effective site for apatite nucleation on its surface. The silanol (Si-OH) groups were known as a promising candidate for supplying effective sites for the apatite nucleation [11]. Once the apatite nuclei have been formed, they spontaneously grow by consuming the Ca^{2+} and P^{5+} from the surrounding fluid, because SBF is already supersaturated with respect to the apatite. Therefore, it is easy to understand that the addition of SiO_2 as well as the increase in its content would enhance the bone-like layer forming ability, since the SiO_2 additive would undoubtedly raise the opportunity for the formation

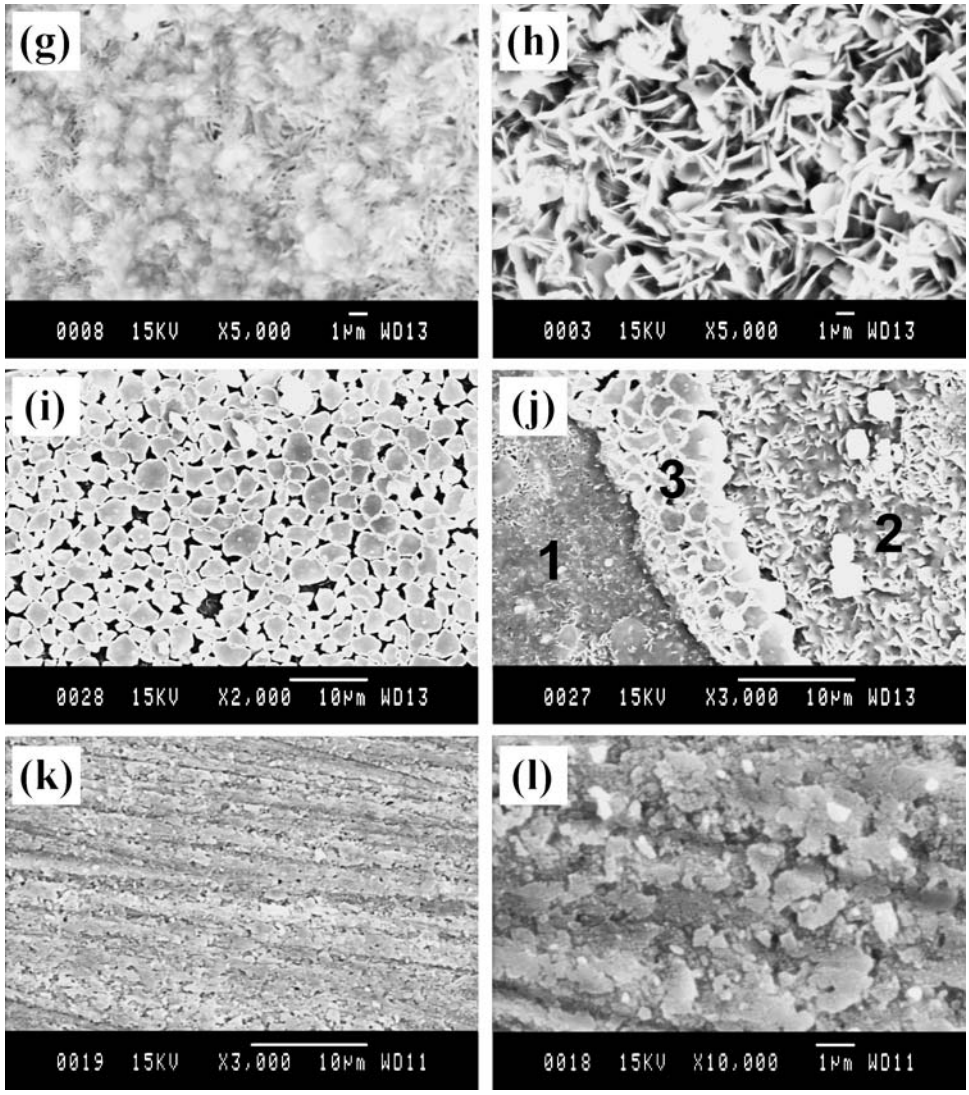

Fig. 6 Continued.

of the silanol groups. Moreover, the progressive addition of SiO_2 promotes the phase transformation from HAp to TCP. It is well known that TCP is a reliable biomaterial having excellent biocompatibility and osteoconductivity, by which formation of new bone is accelerated when the material is immersed into the SBF or implanted into the body, since TCP exhibits higher solubility than HAp [32]. Accordingly, the increase in the content of TCP phase would also speed up the bone-like layer formation. As for the specific case that occurred for the HAp-10 wt.%SiO_2 sample showing an unexpected slow bone-like layer growth, the major reason remains unclear, but might be related with the corresponding microstructures, which revealed an obvious decrease in crystallinity of this material (see Fig. 3(f)). In a word, the formation of the bone-like layer on the surfaces of present bio-composites correlated closely with the increasingly provided silanol groups and transformed TCP phase associated with the content of SiO_2 added.

4. Conclusions

Bioceramic composites were successfully produced by sintering the powders of hydroxyapatite (HAp) mixed directly with additive of 0.5, 1.0, 2.0, 5.0 and 10 wt.%SiO_2, respectively, at 1200°C. Incorporation of Silica into pure HAp brings about a great change in the phase composition, microstructures and bioactivity. The synthesized bio-composites of SiO_2-added HAp consists of crystalline compositions (HAp and TCP) and a glassy phase, and the content of these phases changes greatly with the content of SiO_2 added, thus leading to obvious microstructural changes, for examples, the grain size of HAp decreases with increasing SiO_2 content; as the SiO_2 content increases to 5 wt.%, a distinctive microstructure featuring crystalline clusters with different sizes surrounded by glassy matrix presents. Biomimetic assessments using SBF strongly confirmed that bio-composites of SiO_2-added HAp, especially containing a

higher content of SiO_2 (*e.g.* 5 wt.%), have a markedly more superior bioactivity than that of pure HAp, and this kind of composites can thus be expected to act as a potential synthetic bone material.

Acknowledgments This work was supported by a Grant-in-aid for Scientific Research and Development from the Ministry of Education, Culture, Sports, Science and Technology of Japan The authors also acknowledge the support of "Priority Assistant of the Formation of Worldwide Renowned Centers of Research – The 21st Century COE Program (Project: Center of Excellence for Advanced Structural and Functional Materials Design)" from the Ministry of Education, Culture, Sports, Science and Technology of Japan. Dr. Li is indebted to Mr. M. Aoki for his assistance in soaking experiments, and also to Prof. T. Nakano and Dr. T. Nagase for their helps in various respects.

References

1. M. J. YASZEMSKI, R. G. PAYNE, W. C. HAYES, R. LANGER and A. G. MIKOS, *Biomaterials* **17** (1996) 175.
2. M. JARCHO, C. H. BOLEN, M. B. THOMAS, J. BOBICK, J. F. KAY and R. H. DOREMUS, *J. Mater. Sci.* **11** (1976) 2027.
3. G. DEWITH, H. J. A. VANDIJK, N. HATTU and K. PRIJS, *J. Mater. Sci.* **16** (1981) 1592.
4. J. C. ELLIOTT, in "Structure and Chemistry of the Apatite and Other Calcium Orthophosphates" (Elservier Press, Amsterdam 1994) p. 1–62.
5. C. P. A. T. KLEIN, A. A. DRIESSEN, K. DE GROOT and A. VAN DEN HOOF, *J. Biomed. Mater. Res.* **17** (1983) 769.
6. E. SCHEPERS, M. DECLERCQ, P. DUCHEYNE, R. KEMPENEERS, *J. Oral. Rehab*. **18** (1991) 439.
7. P. DUCHEYNE and Q. QIU, *Biomaterials* **20** (1999) 2287.
8. E. M. CARLISLE, *Science* **167** (1970) 279.
9. L. L. HENCH, *J. Am. Ceram. Soc.* **74** (1991) 1487.
10. L. L. HENCH, *J. Am. Ceram. Soc.* **81** (1998) 1705.
11. T. KOKUBO, *Acta Mater.* **46** (1998) 2519.
12. S. HAYAKAWA, K. TSURU, C. OHTSUKI and A. OSAKA, *J. Am. Ceram. Soc.* **82** (1999) 2155.
13. M. VALLET-REGI, A. M. ROMERO, C. V. RAGEL and R. Z. LEGEROS, *J. Biomed. Mater. Res.* **44** (1999) 416.
14. T. KASUGA, Y. HOSOI and M. NOGAMI, *J. Am. Ceram. Soc.* **84** (2001) 450.
15. C. A. MILLER, T. KOKUBO, I. M. REANEY, P. V. HATTON and P. F. JAMES, *J. Biomed. Mater. Res.* **59** (2001) 473.
16. T. KOKUBO, H. Y. KIM and M. KAWASHITA, *Biomaterials* **24** (2003) 2161.
17. A. J. RUYS, *J. Austral. Ceram. Soc.* **29** (1993) 71.
18. S. R. KIM, D. H. RIU, Y. J. LEE and Y. H. KIM, *Key Eng. Mater.* **218–220** (2002) 85.
19. S. R. KIM, J. H. LEE, Y. T. KIM, D. H. RIU, S. J. JUNG, Y. J. LEE, S. C. CHUNG and Y. H. KIM, *Biomaterials* **24** (2003) 1389.
20. I. R. GIBSON, S. M. BEST and W. BONFIELD, *J. Biomed. Mater. Res.* **44** (1999) 422.
21. I. R. GIBSON, S. M. BEST and W. BONFIELD, *J. Am. Ceram. Soc.* **85** (2002) 2771.
22. S. D. LANGSTAFF, M. SAYER, T. J. N. SMITH and S. M. PUGH, *Mater. Res. Soc. Symp. Proc.* **550** (1999) 1727.
23. S. D. LANGSTAFF, M. SAYER, T. J. N. SMITH, S. M. PUGH, S. A. M. HESP and W. T. THOMPSON, *Biomaterials* **20** (1999) 1727.
24. S. D. LANGSTAFF, M. SAYER, T. J. N. SMITH and S. M. PUGH, *Biomaterials* **22** (2001) 135.
25. M. SAYER, A. D. STRATILATOV, J. REID, L. CALDERIN, M. J. STOTT, X. YIN, M. MACKENZIE, T. J. N. SMITH, J. A. HENDRY and S. D. LANGSTAFF, *Biomaterials* **24** (2003) 369.
26. J. W. REID, A. PIETAK, M. SAYER, D. DUNFIELD and T. J. N. SMITH, *Biomaterials* **26** (2005) 2887.
27. T. KOKUBO, H. KUSHITANI, S. SAKKA, T. KITSUGI and T. YAMAMUTO, *J. Biomed. Mater. Res.* **24** (1990) 721.
28. T. KOKUBO, S. ITO, Z. T. HUANG, T. HAYASHI, S. SAKKA, T. KITSUGI and T. YAMAMUTO, *J. Biomed. Mater. Res.* **24** (1990) 331.
29. C. OHTSUKI, H. KUSHITANI, T. KOKUBO, S. KOTANI and T. YAMAMURO, *J. Biomed. Mater. Res.* **25** (1991) 1363.
30. C. OHTSUKI, T. KOKUBO and T. YAMAMURO, *J. Mater. Sci.: Mater. Med.* **3** (1992) 119.
31. T. KOKUBO, H. –M. KIM, M. KAWASHITA and T. NAKAMURA, *J. Mater. Sci.: Mater. Med.* **15** (2004) 99.
32. F. H. LIN, C. J. LIAO, K. S. CHEN, J. S. SUN and C. P. LIN, *Biomaterials* **22** (2001) 2981.